SMART Sensors for Cell Growth Monitoring in Closed System G-Rex for Scalable, Cost-Conscious Cell and Gene Therapy Manufacturing

Subhanwit Roy[1], Samuel Rothstein[1], Aidan Shervheim[1], Yee Jher Chan[1], Cameron Greenwalt[1], Nathan Neihart[1], Jose Juarez[2], Patricia Turner[2], Dan Welch[3], John Wilson[2,3], Daniel Fick[2,3], and Nigel F. Reuel[1]*

1. Skroot Laboratory Inc. – Ames, Iowa
2. CellReady LLC – Houston, Texas
3. Wilson Wolf Manufacturing LLC – St. Paul, Minnesota

* Corresponding Author – reuel@skrootlab.com

Table of Contents

Supplement 1: SMART Sensor Response to T Cell-Secreted Signaling Molecules

T cells are known to secrete lipid mediators derived from polyunsaturated fatty acids (PUFAs), specifically eicosanoids and their derivatives, such as prostanoids (like PGE_2) and leukotrienes. These signaling lipids function as key modulators of immune responses, influencing T cell functions like migration and differentiation. Arachidonic acid (AA), an omega-6 PUFA that is essential for cell membrane structure and a source of energy, serves as a precursor to eicosanoids.

To validate the SMART sensor transduction method for T cells, an experiment was performed using two 35 mm petri dishes (control and experimental) with embedded SMART sensors. Each dish was initially filled with 3 mL phosphate-buffered saline (PBS) to establish a 5 hour long baseline response using SMART readers in continuous mode. Subsequently, 0.25 mL of an AA solution (100 mg AA dissolved in 1 mL ethanol) was added to the experimental petri dish, while 0.25 mL of pure ethanol was added to the control. As shown in **Figs. S1-1a** and **S1-1b**, AA addition produced a distinct change in sensor response compared to the control. A second addition of 0.75 mL of the AA solution to the experimental dish, paired with 0.75 mL ethanol to the control, induced a further pronounced response, demonstrating the sensitivity of the SMART sensor transduction method to AA, a precursor of T cell-derived lipid mediators.

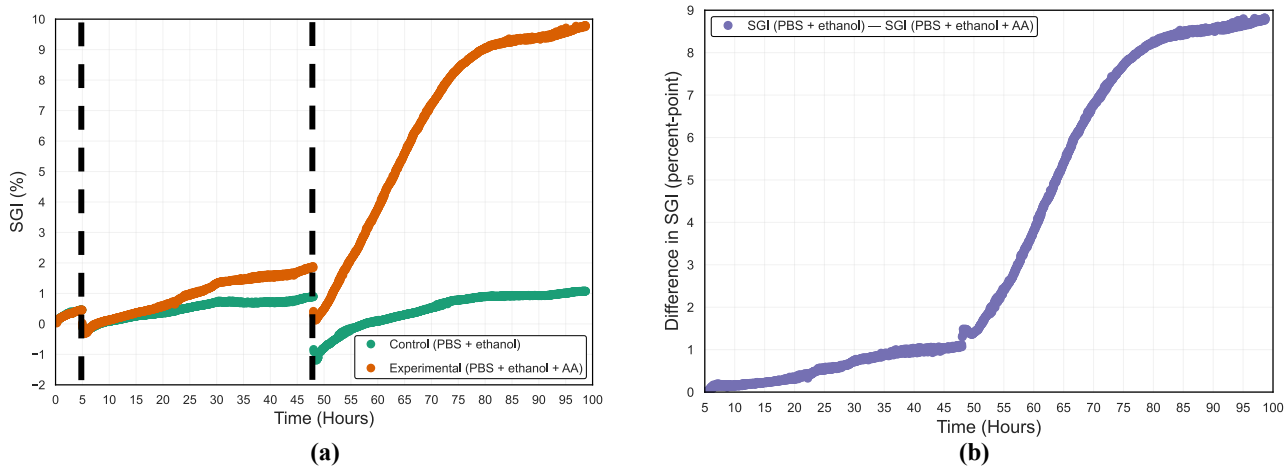

Figure S1-1 – (a) SMART sensor response for control and experimental petri dishes showing clear effect of Arachidonic Acid (AA). The two vertical dashed black lines correspond to instances of addition of chemicals to the dishes. (b) Difference in sensor response between two dishes, from the point of first chemical addition, further emphasizing the transduction of the sensor by AA. Note that this plotted difference is simply one SGI plot subtracted from another, and is different from the quantity dSGI, which indicates the finite time derivative of SGI.

Supplement 2: Effect of Kerf on Sensor Response

In this work, the PET layer in the sensor stack was laser cut to form high-precision air voids that enabled the transduction membrane (softened in response to secondary metabolites in the cell culture) to collapse and fill the voids, thereby altering the resonant sensor's response, quantified in terms of the Skroot Growth Index (SGI). The cross section stack of the sensor is revisited in **Fig. S2-1a**.

It was observed that changing the kerf setting on the laser cutter, which controls the width of the PET material removed, significantly affected the saturation behavior of the SMART sensor. In particular, a wider kerf resulted in a greater overall shift in SGI and a faster saturation to the final value. **Figs. S2-1b** and **S2-1c** illustrate this effect for *E. coli* and CAR-T cell cultures, respectively.

Thus, kerf width represents a useful design parameter for tuning sensor response to track cell growth metrics of interest. Herein, a nominal kerf width of 300 µm was ultimately selected as a trade-off between the sensor's ability to track lactate (see the 350 µm trace in **Fig S2-1c**) and the tolerance limitations of the third-party sensor manufacturer.

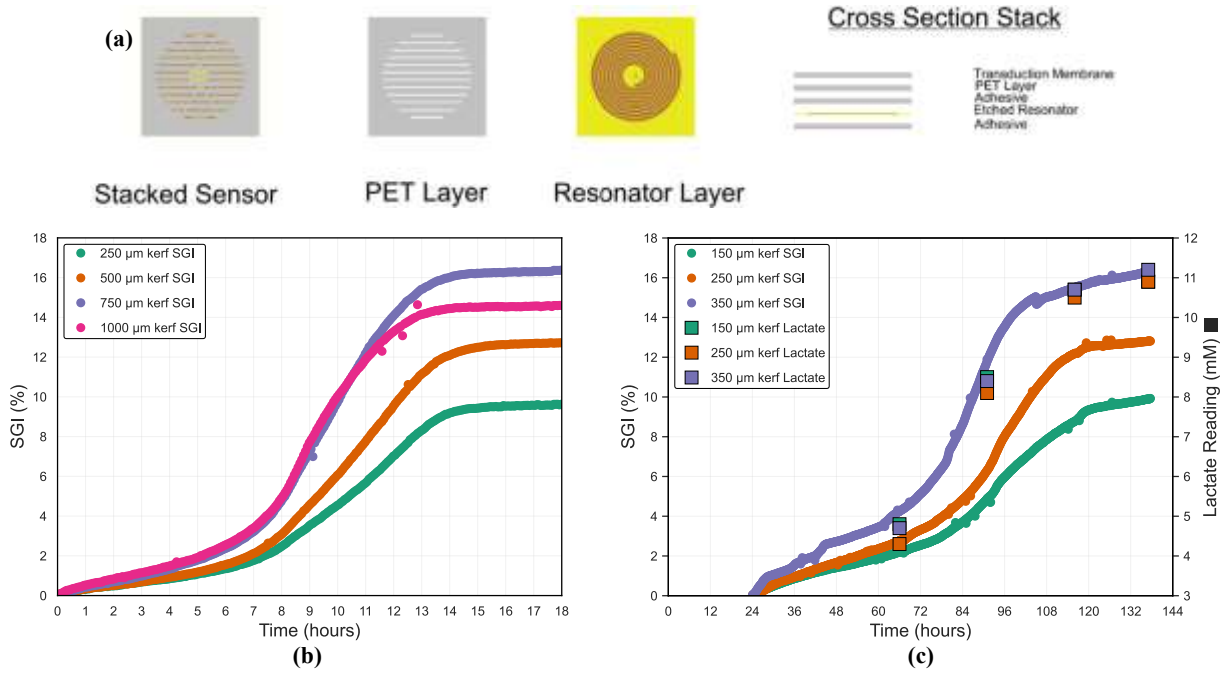

Figure S2-1 – (a) Cross-sectional stack of the SMART sensor, highlighting the cut channels in the PET layer. The channel width (kerf) is a tunable design parameter that modulates sensor response. This effect is demonstrated in (b) E. coli and (c) CAR-T cultures, where larger kerf widths result in greater SGI shifts and faster saturation dynamics.

Supplement 3: Cytotoxicity Testing and Accelerated Aging Testing for Third-party Sensors

Cytotoxicity Testing

A cytotoxicity assay was conducted on the SMART sensors adhered to polycarbonate caps (same material as the G-Rex 100M body) by NAMSA. The study was performed in accordance with ISO 10993-5 and BS EN ISO 10993-5, which specify tests for in vitro cytotoxicity of medical devices, and adhered to FDA Good Laboratory Practice (GLP) Regulations (21 CFR, Part 58)

For the evaluation, a single preparation of the Cap with Sensor was extracted in Eagle's Minimal Essential Medium supplemented with 5% Fetal Bovine Serum (EMEM 5% FBS) at 37 °C for 24 hours with continuous agitation. The chosen extraction vehicle was designed to optimize the extraction of both polar and non-polar components from the test article. Triplicate monolayers of L-929 mouse fibroblast cells, a historically used and established cell line sensitive to cytotoxic leachates, were then dosed with the prepared extract. These cell monolayers were subsequently incubated at 37 °C in 5% CO_2 for 72 hours, after which they were microscopically examined for any signs of abnormal cell morphology or cellular degeneration. Reactivity was graded on a scale from 0 (none) to 4 (severe).

The validity of the assay was confirmed by the performance of the control articles. The negative control (High density polyethylene) and the vehicle control (EMEM 5% FBS) both exhibited no reactivity, receiving a grade of 0. Conversely, the positive control (0.1% Zinc diethyldithiocarbamate) demonstrated severe cytotoxicity, consistently scoring a grade of 4.

The test article extract showed no evidence of causing cell lysis or toxicity in any of the test wells at 72 hours. All three replicates of the received a reactivity grade of 0 (None). This result indicates that the test article extract met the requirements of the test, as its biological response was well within the acceptable limit of less than or equal to a grade 2 (mild reactivity). The conclusions drawn are specific to the test article evaluated in this study.

Accelerated Aging Testing

Four SMART sensors were applied to each G-Rex 100M device which were then gamma sterilized. Subsequently, the G-Rex 100M devices were split into four different aging groups – Year 0 through Year 3. While the Year 0 devices were stored at room temperature, the other groups thermally aged inside a Fisherbrand™ Gravity Oven at Skroot Laboratory, Inc. for a predetermined time for each aging group calculated using Accelerated Aging Theory[1]:

$$t_{accelerated} = \frac{t_{desired}}{Q_{10}^{(T_{elevated} - T_{ambient})/10}} \quad \text{(S3-1)}$$

where $t_{accelerated}$ and $t_{desired}$ respectively denote, the accelerated aging and desired real time aging time durations, Q_{10} is a constant with value 2.0, while $T_{elevated}$ and $T_{ambient}$ are the elevated and ambient temperatures respectively. Using $T_{elevated}$ as 59 °C and $T_{ambient}$ as 22 °C, resulted in the following accelerated aging time durations for each aging group.

Table S3-1 – Sensor Aging Group and Accelerated Aging Time Duration for Each G-Rex 100M Used for Aging Test

G-Rex 100M Identifier	No. of Sensors	Sensor Aging Group (Years)	Accelerated Aging Time Duration (Days)
V-0144	4	0	0
V-0147	4	1	28
V-0150	4	2	56
V-0153	4	3	84

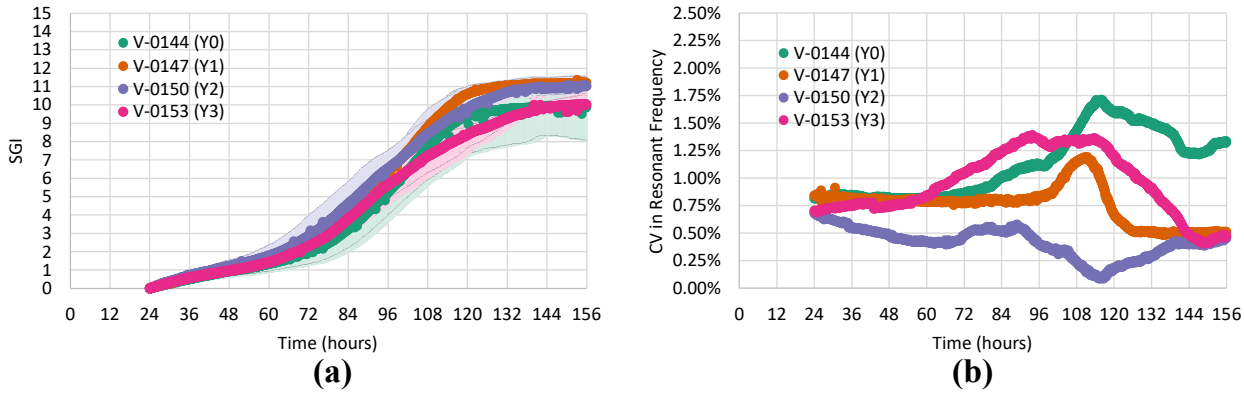

Figure S3-1 – (a) Mean SGI with min and max error bars (denoted by tinting the primary color) for G-Rex 100M devices aged 0 through 4 years, (b) coefficient of variation (CV) in resonant frequency measurements for the 4 G-Rex devices.

[1] Hemmerich, K. J., "General Aging Theory and Simplified Protocol for Accelerated Aging of Medical Devices," Medical Plastics and Biomaterials, July/August 1998, pp. 16–23.

Upon completion of accelerated aging for each aging group, the G-Rex 100M devices were stored at room temperature until all groups were done aging.

The cell culture test involved placement of the G-Rex 100Ms on Skroot readers. Cell seeding was done on Day 0 using the medium growth condition (as defined in the main text) from the same PBMC bag for all G-Rex 100M devices.

Aging over a 3-year period did not adversely impact sensor reliability, cell growth tracking, or data quality (**Fig. S3-1 a, b**). These findings support the use of Skroot sensors for long-term storage without compromising downstream biomanufacturing performance.

Supplement 4: Analysis of Raw Reader Signal to Compute SGI

For every frequency sweep, the reader hardware interrogates the sensor-under-test wirelessly at each frequency point in the sweep and outputs a digitally converted DC voltage value. This DC voltage versus interrogation frequency curve peaks when the interrogation frequency is equal to the resonant frequency of the sensor. To account for the reader's intrinsic frequency response and cancel off any systematic errors, each frequency sweep of the sensor is calibrated against a reader-only calibration response (no sensor present) done before the start of each experiment. **Fig. S-4-1a** demonstrates a sample calibration response, while **Fig. S-4-1b** shows the calibrated sensor response (signal strength) for the first and last frequency sweeps from a 7-day long cell culture run with a SMART sensor. The calibrated sensor response at each frequency point (f) is calculated in software as the following and expressed in percentage form:

$$V_{sensor,calibrated}(f) = \left(\frac{V_{sensor,raw}(f)}{V_{calibration}(f)} - 1\right) \quad \text{(S3-1)}$$

where $V_{sensor,calibrated}$ and $V_{sensor,raw}$ represent the calibrated and raw sensor outputs, respectively, with $V_{calibration}$ being the reader-only calibration response. The calibrated sensor output is a measure of the percent change in the strength of the output signal influenced by the sensor on top of the baseline calibration response, and is thus termed as signal strength. Major factors which impact signal strength include the coupling coefficient between the reader antenna and the conductive losses in the media and a lower signal strength makes it harder to detect the resonant peak due to the sensor.

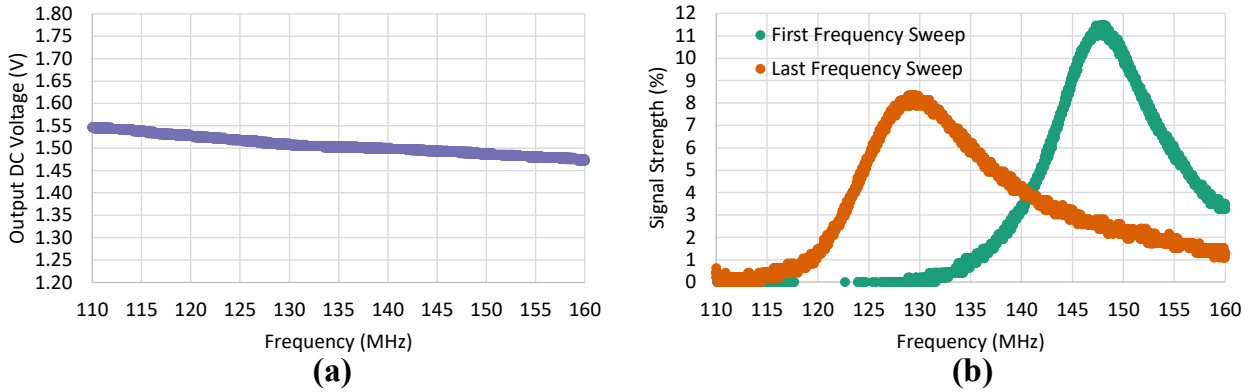

Figure S4-1 – (a) Calibration response of reader hardware showing output DC voltage over an entire frequency sweep, (b) calibrated sensor response from the first and last frequency sweep of a 7-day long cell culture run clearly showing the shift in resonant (peak) frequency.

The peak itself is extracted by fitting a 500-point Gaussian curve around the absolute maximum and the corresponding interrogation frequency point is regarded as the sensor resonant frequency, from which the software can readily calculate SGI using equation (1) from the main text. Using this formulation, in **Fig. S-4-1b**, given that the first and last frequency sweeps yield resonant frequencies of 147.29 MHz and 128.86 MHz respectively, the total SGI shift (assuming an equilibration time of 0) is $(147.29 - 128.86)/128.86 = 12.51\%$.

Finally, a Savitzky-Golay digital filter[2] is to smooth the real-time SGI curve.

[2] Schafer, R. W., "What Is a Savitzky-Golay Filter? [Lecture Notes]," *IEEE Signal Processing Magazine*, vol. 28, no. 4, 2011, pp. 111–117.

Supplement 5: Effect of Reader Temperature on Cell Growth

During the early development phase of the Skroot platform, a commercial portable vector network analyzer (VNA) was used to interrogate the SMART sensor. However, it was observed that G-Rex devices with active readers resulted in a lower harvest cell count compared to control vessels not using Skroot technology (**Fig. S5-1a**), without an observable change in cell viability (**Fig. S5-1b**). Temperature measurements (**Fig. S5-1c**) showed a ~1 °C increase when using Skroot readers leading to the hypothesis that the heat generated by the VNA was increasing the temperature and hindering cell growth.

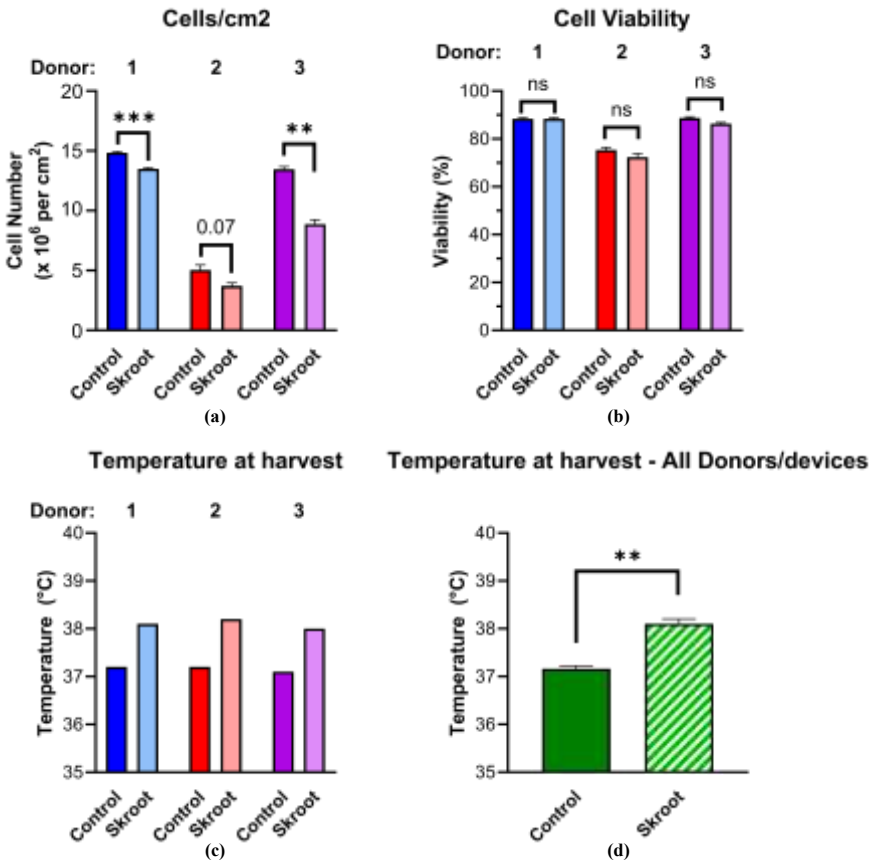

Figure S5-1 – (a) Comparison of cell count in control versus early-stage Skroot G-Rex devices (with active VNA readers) showing lower harvest cell count across three cell cultures with independent donors with the early-stage Skroot platform (b) without a significant drop in viability. (c) The temperature of the vessel upon harvest was consistently greater by ~1 °C for devices using the Skroot platform, (d) characterized further by the average temperature measurement.

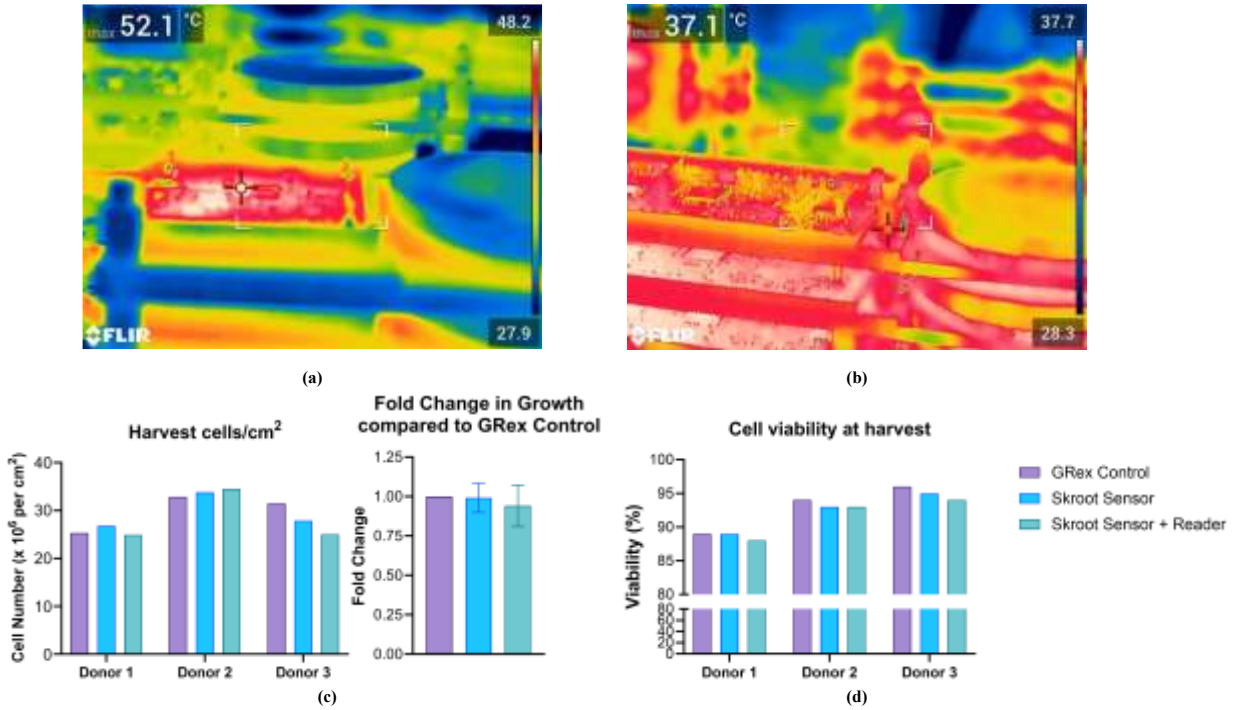

Figure S5-2 – Thermal images to compare the temperature of the (a) commercial VNA reader and (b) custom-designed reader showing that the custom-designed reader did not heat up like the VNA over the course of its operation. Cell testing with the new custom-designed reader demonstrated no statistically significant difference from control G-Rex devices in terms of (c) cell count and (d) cell viability upon harvest.

This hypothesis led us to swap the VNA with a custom-designed reader which had careful hardware and firmware design to manage the heat generated by the system. In particular, special attention was paid to the power consumption of electronic components selected for the design, while the firmware on the custom-designed reader ensured that the hardware was put to sleep when not actively scanning sensors which stopped the incubator interior from heating up due to reader operation. Thermal images comparing the VNA (**Fig. S5-2a**) and the custom-designed reader (**Fig. S5-2b**) showed that the hottest part of the latter was significantly lower (and approximately the ambient incubator temperature).

Finally, we investigated if there was any statistically significant effect of the reader on final harvest cell count (**Fig. S5-2c**) or viability (**Fig. S5-2d**) compared to control G-Rex devices. Statistical comparisons were performed using a two-way analysis of variance (ANOVA) with *Device* (three levels: G-Rex Control, Skroot Sensor, and Skroot Sensor + Reader) and *Donor* (three levels: Donor 1, Donor 2, and Donor 3) as fixed factors. Bonferroni's multiple-comparison correction was applied to post-hoc pairwise *t*-tests to control for multiple testing.

For final cell count, the *Device* term was not significant ($p = 0.65$), indicating no measurable difference in harvest cell count across vessel conditions. The *Donor* term was significant ($p = 0.027$), reflecting expected biological variation among donors. Pairwise Bonferroni-adjusted *p*-values for all device comparisons were 1.0, confirming the absence of device-dependent effects.

For viability at harvest, the ANOVA identified a statistically significant *Device* effect ($p = 0.04$) and a highly significant *Donor* effect ($p < 0.001$). However, Bonferroni-adjusted post-hoc comparisons between individual device groups yielded adjusted *p*-values of 1.0, indicating that no pairwise differences were significant after correction. The adjusted *p*-value calculations are presented in **Table S5-1**.

Collectively, these analyses confirm that neither the presence of the sensor nor measurement using the cooler hardware affected cell growth or viability at harvest.

Table S5-1 – Pairwise comparisons between device conditions. Means represent averages across three donors per device condition. Bonferroni correction applied for three pairwise tests per outcome ($m = 3$); Bonferroni-adjusted p=1.00 indicates no significant difference at $\alpha = 0.05$.

Comparison	Outcome	Mean (Group 1)	Mean (Group 2)	*p* (raw)	*p* (Bonferroni-adjusted)
GRex Control vs Skroot Sensor	**Cell count**	30.1	29.8	0.92	**1.00**
GRex Control vs Skroot Sensor + Reader	**Cell count**	30.1	28.7	0.69	**1.00**
Skroot Sensor vs Skroot Sensor + Reader	**Cell count**	29.8	28.7	0.75	**1.00**
GRex Control vs Skroot Sensor	**Viability (%)**	92.9	92.3	0.82	**1.00**
GRex Control vs Skroot Sensor + Reader	**Viability (%)**	92.9	91.6	0.65	**1.00**
Skroot Sensor vs Skroot Sensor + Reader	**Viability (%)**	92.3	91.6	0.80	**1.00**

Supplement 6: SMART Platform Validation Across Cell Types

The SMART sensor platform was validated across multiple cell types, including fast-growing bacteria and yeast as well as slower-growing mammalian cells such as CHO and K-562 in addition to CAR-T as discussed in the main text. The sensors successfully tracked cell growth in both static and dynamic culture vessels, with sensor outputs benchmarked against standard manual sampling parameters (**Figs. S6-1a–c**). Furthermore, the sensors demonstrated the ability to noninvasively detect aberrant cell culture conditions such as contamination. As shown in **Fig. S6-1d**, contamination induced a rapid increase in SGI followed by early signal saturation, highlighting the platform's potential for real-time contamination detection. Future work analyzing the derivative of SGI may enable development of a robust, continuous contamination monitoring tool.

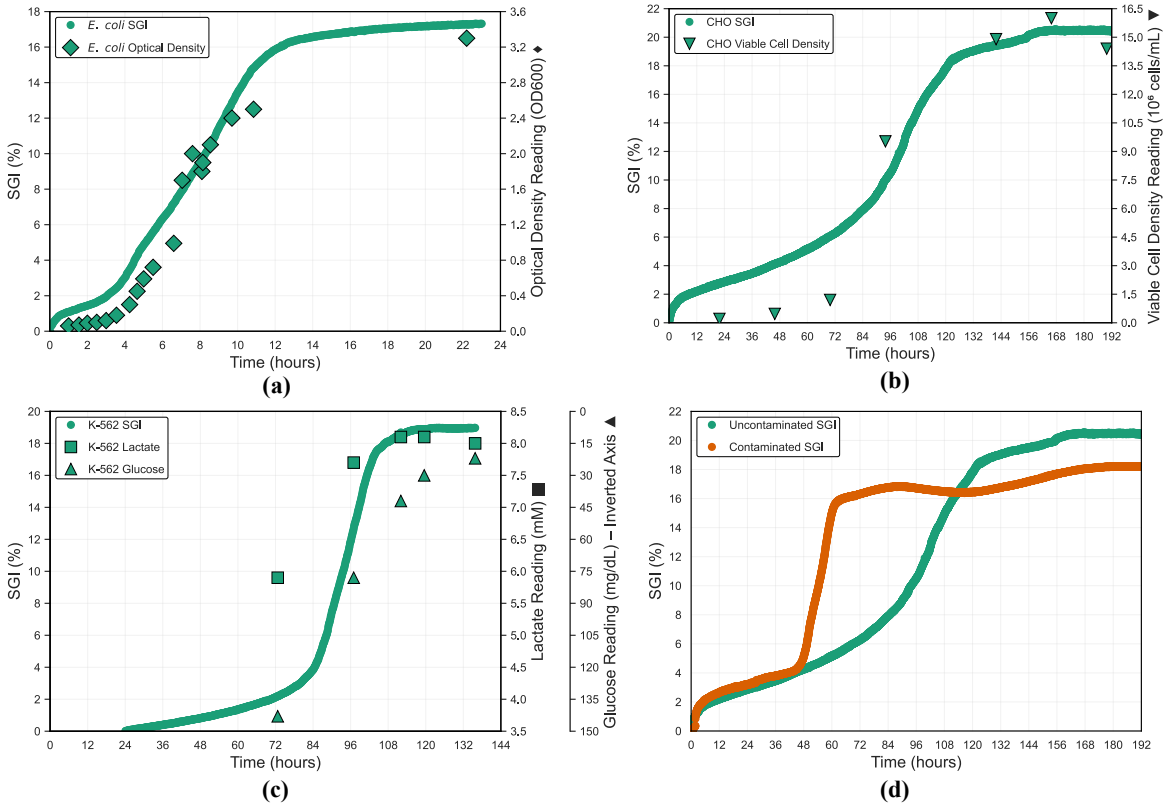

Figure S6-1 – SMART sensor response for three representative cell types: (a) E. coli cultured in a 250 mL shake flask, with SGI compared to manually sampled optical density (OD600); (b) CHO cells cultured in a 250 mL shake flask, with SGI compared to manually sampled viable cell density; (c) K-562 cells cultured in a G-Rex 100M, with SGI compared to manually sampled lactate and glucose concentrations (glucose plotted with an inverted right axis); along with (d) comparison of SMART sensor response in uncontaminated and contaminated CHO cell cultures grown in 250 mL shake flasks. Contamination resulted in a rapid rise in SGI followed by early saturation.

Supplement 7: Harvest Indicator Validation

Herein we provide an example of a simple binary "go/no-go" (ready for harvest/not ready for harvest) indicator based on benchtop reader data. An experiment was conducted at

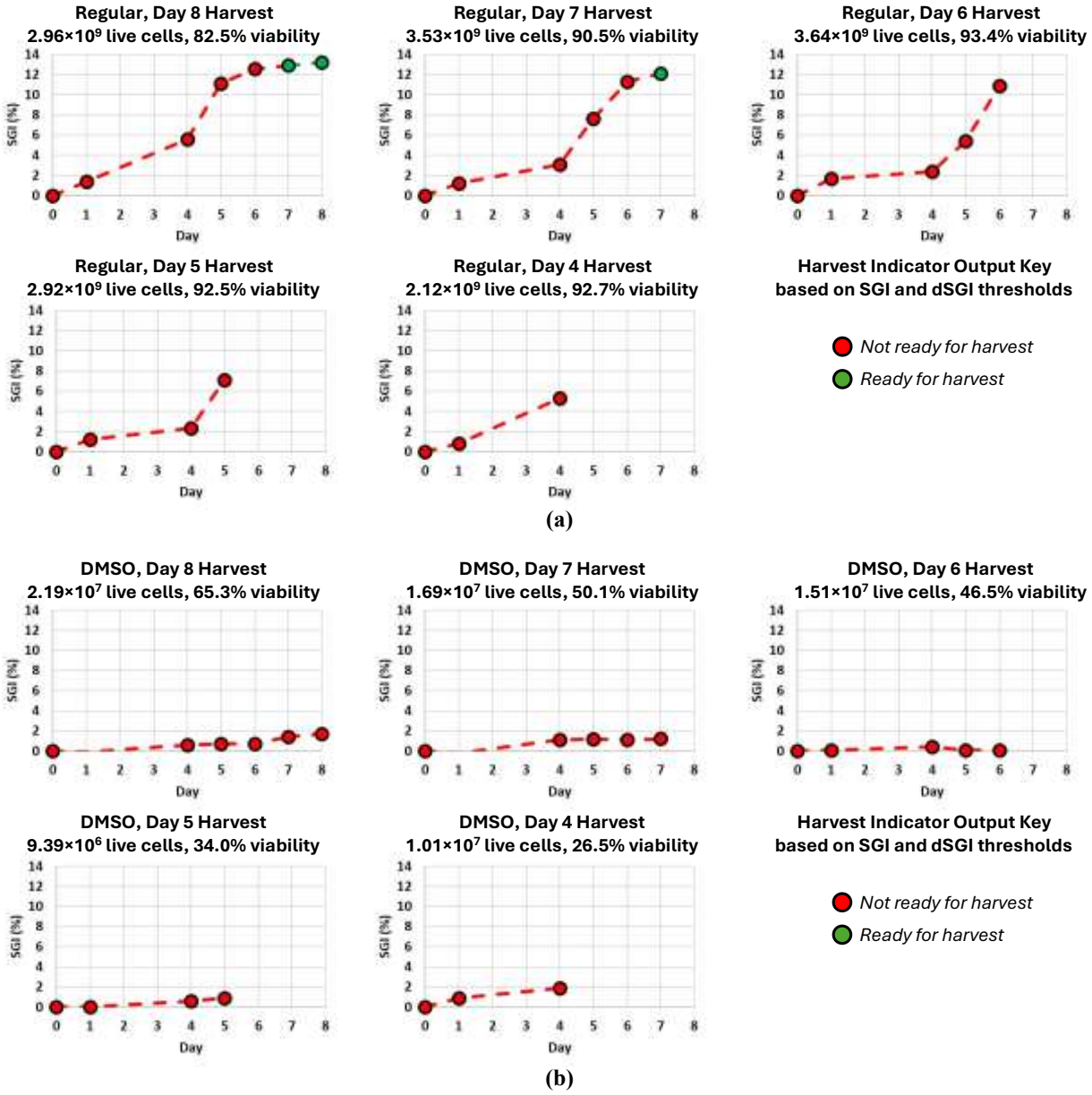

Figure S8-1 – (a) SMART sensor response using benchtop reader for 5 G-Rex 100M devices that were identically seeded with 50 million cells on the same day (Day 0), activated together, and harvested on Days 8, 7, 6, 5, and 4 along with the binary "go/no-go" output of the harvest indicator. (b) The same set of plots for 5 G-Rex 100M devices that were additionally spiked with 10 mL 2.5% DMSO solution to stunt cell growth. Corresponding to each vessel, also shown are terminal live cell count and viability. It is evident that the harvest indicator successfully recommended harvest in the window with the highest live cell count.

CellReady involving 10 G-Rex 100M devices – all seeded on the same day (Day 0), identically, with 50 million cells from a PBMC bag. The 10 vessels were equally split into two groups – one which was allowed to grow using CellReady's standard protocol while the other had each vessel spiked with 10 mL of a 2.5% dimethyl sulfoxide (DMSO) solution to stunt cell growth. For each group, the 5 vessels were harvested successively on Days 4 through 8. On each day, SMART reader (in benchtop mode) scans were taken along with manual samples for lactate and glucose for all active vessels, while terminal cell count and viability were recorded upon harvest. The reader implemented a real-time harvest indicator algorithm based on a decision rule using thresholds of SGI > 7% and dSGI < 0.05 percentage points per hour (as described in **Fig. 5**). The performance of the harvest indicator was validated against the terminal live cell count and it was found that the indicator was successfully triggered only when live cell count was the highest (**Fig. S8-1a**). The only scope of improvement was early detection of the regular vessel harvested on Day 6 – finer resolution provided by more frequent/continuous reader scan could have facilitated it. Nevertheless, it can be inferred from the Day 7 harvest vessel, that had the Day 6 harvest vessel been run for an extra day, the harvest indicator would have been triggered with the live cell count still sufficiently high.

Moreover, with the stunted growth condition (DMSO), no false positives were observed – further corroborating the effectiveness of the harvest indicator. Additionally, the DMSO

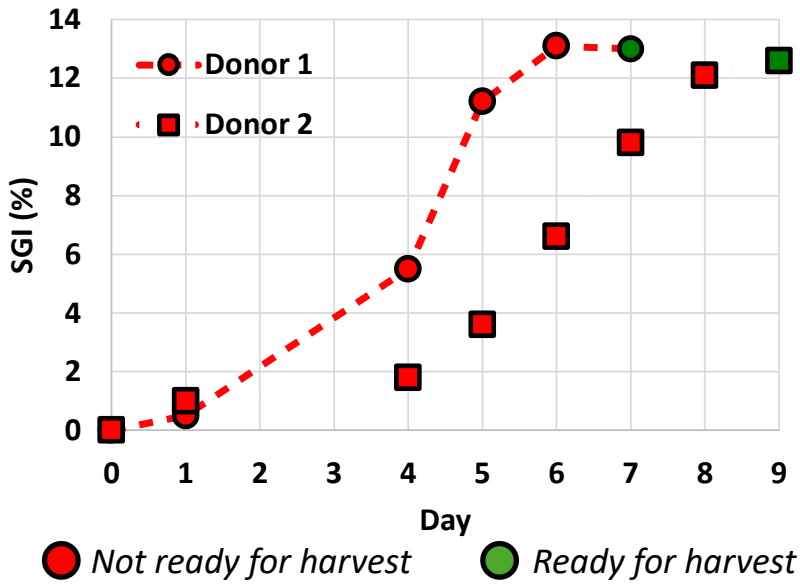

Figure S7-2 – SMART sensor response using benchtop reader for 2 G-Rex 100M devices that were seeded with 50 million cells from two different donors on the same day (Day 0), activated together, and harvested upon the triggering of the harvest indicator. Both vessels yielded more than 3×10^9 viable cells upon their harvest on Day 7 and Day 9 respectively.

vessels also point toward the possibility of implementing a threshold for early detection of slow or abnormal growth which could enable a manufacturing facility to intervene and course correct.

Finally, the inverse problem (reader-driven harvest instead of fixed harvests) was validated by seeding two G-Rex 100M devices with the equal number of cells but from two different donors (Donor 1 and Donor 2) and harvesting them based on the benchtop reader's harvest indicator output (**Fig. S7-2**). The cells from Donor 1 expanded more rapidly, triggering the harvest indicator at Day 7 and yielding 3.77×10^9 viable cells at 87.4% viability upon harvest, whereas the Donor 2 vessel was recommended for harvest on Day 9, producing 3.42×10^9 viable cells at 89.3% viability. On Day 7, manual glucose measurements confirmed that glucose in the Donor 1 vessel was completely depleted, while 63 mg/dL remained in Donor 2, which was fully consumed by Day 9. A fixed harvest on Day 7 would have produced a sub-optimal yield for Donor 2. These results demonstrate that the SMART G-Rex's data-driven harvest recommendation accurately tracked both cell growth and nutrient utilization, highlighting its potential in maximizing viable cell count in a CGT production process while eliminating the need for regular manual sampling.

Supplement 8: Harvest Indicator Setup Guide

Supplement 7 demonstrated a successful implementation of the SMART benchtop reader's harvest indicator. However, the thresholds used by the indicator were specific to that use-case and are not expected to universally apply across different cell types, media formulations, or seeding and activation protocols. To make the real-time decision logic transferable across laboratories and manufacturing facilities, we provide below a simplified workflow to determine site-specific thresholds for SGI and dSGI.

Logic Overview

The SMART benchtop reader harvest indicator combines two parameters – the measured Sensor Growth Index (SGI) and its calculated rate of change (dSGI) to recommend the optimal harvest window. The indicator is triggered when SGI plateaus above a predefined threshold (minimizing false positives) and dSGI approaches zero, signifying that cell expansion has reached its peak.

Harvest Threshold Setup and Tuning Procedure

1. Select a representative process
    - Choose a cell line and culture protocol with a well-defined growth pattern and known optimal harvest day (maximum viable cell density or functional yield) that reflects the intended use-case.
2. Prepare replicate vessels
    - Run three or more SMART G-Rex cultures in parallel under identical conditions. Collect daily benchtop-reader scans (≈ 24-h intervals).
3. Staggered harvests
    - Harvest separate vessels one day before, on, and one day after the expected optimum. Record terminal live-cell counts and viability.
    - If running more than three replicates, either harvest multiple vessels on these three days to increase confidence in the thresholds, or include additional harvests (e.g., ±2 days from the optimal day) to broaden the time range of inquiry
4. Estimate thresholds
    - Plot the SGI and dSGI (one-day slope) time-series.
    - Identify the SGI value on the optimal harvest day (candidate τ_{SGI}) and the corresponding 24-h dSGI (called τ_{dSGI}).
    - The pair (τ_{SGI}, τ_{dSGI}) defines the provisional *"ready for harvest"* rule: **SGI ≥ τ_{SGI} and dSGI ≤ τ_{dSGI}**

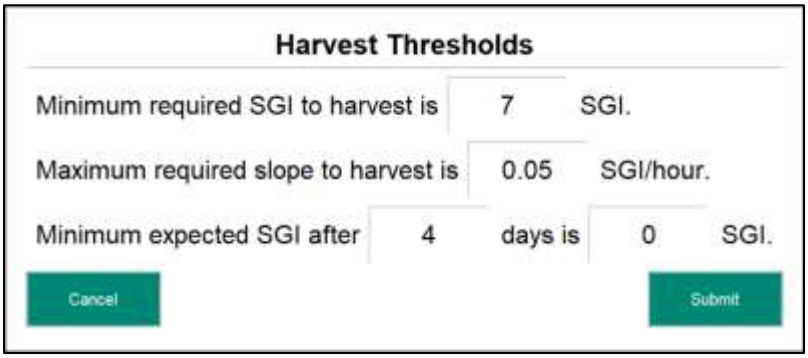

Figure S8-1 – In-app settings window on benchtop reader to program harvest indicator thresholds showing example values

5. Refinement
    - Repeat the experiment across at least three independent runs to confirm repeatability and adjust thresholds according to desired sensitivity (earlier = conservative; later = aggressive).
6. Validation and Continual Refinement
    - Validate the finalized thresholds across multiple donors or process variants. The rule should trigger within the window yielding maximal viable cell count while remaining inactive under sub-optimal or growth-stunted conditions.
    - Continual Refinement: Continue to refine thresholds using data from validation and production runs as needed.
7. Aberrant growth detection
    - Optionally define a day-specific SGI threshold $\tau_{SGI,aberrant}$ to flag atypical growth behavior:
    - On Day *d*, if SGI < $\tau_{SGI,aberrant}$, indicate *"aberrant growth"*

Fig. S8-1 illustrates a window on the benchtop reader app with settings used for experiments discussed in Supplement 7. According to these settings:

- Harvest would be triggered only when SGI crosses 7% and dSGI falls under 0.05 percentage points per hour.
- Aberrant growth threshold was set to 0 SGI on Day 4. This is a really conservative threshold as it would only flag a negative SGI as aberrant.

Supplement 9: Harvest Predictor Proof-of-Concept

This supplement shows the proof-of-concept for developing a real-time harvest predictor based on continuous SMART sensor data. **Fig. S9-1** illustrates SGI and dSGI for a K562 culture demonstrated above. The data received up to time = 100 h was used to predict when SGI would saturate in terms of dSGI falling under a predetermined threshold (similar to the harvest indicator discussed in the main text). For this particular use case, a Gaussian fit around the critical growth rate (peak in dSGI) was used with a dSGI threshold of 0.05 percent-point/hour, resulting in a saturation prediction 8 hours in advance. The sensor response post 100 hours shows the predicted harvest window indeed corresponded with the beginning of SGI saturation. The prediction would continue to be refined as more incoming data was processed in real-time beyond the 100 hour mark.

Future research would involve incorporating a robust machine learning algorithm, in accordance with application-specific calibration inputs, to accurately predict harvest readiness in mammalian cells at least 24 hours ahead of time.

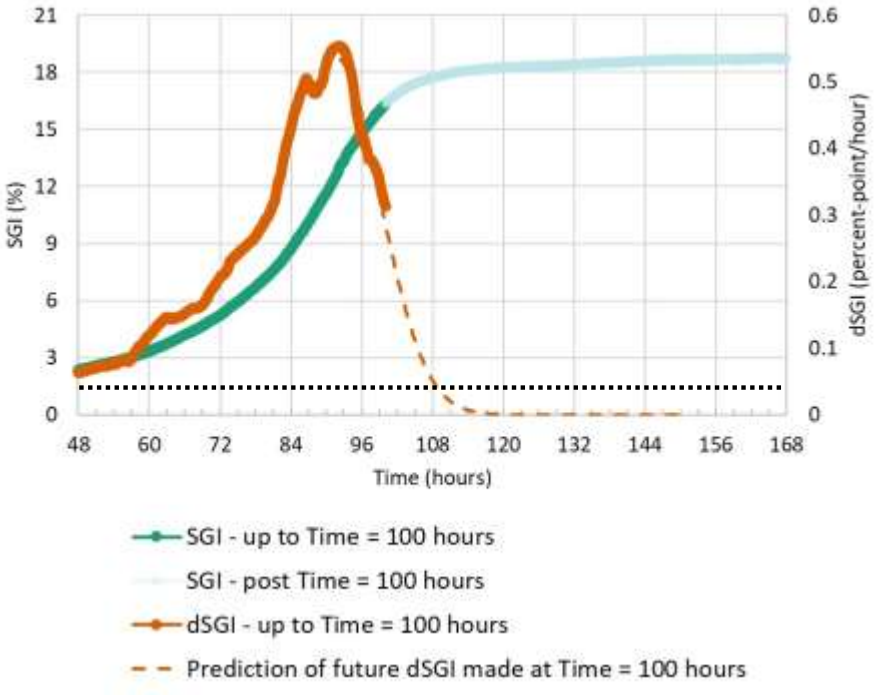

Figure S9-1 – SGI and dSGI for K562 culture in T flask. Data up to 100 hours was used to predict dSGI falling lower than a predetermined threshold of 0.5 percent-points/hour. The SGI data post 100 hours demonstrate the accuracy of the prediction.